Published in final edited form as:

Metallomics. 2020 March 25; 12(3): 346–362. doi:10.1039/c9mt00301k.

Remodeling of Zn^{2+} Homeostasis Upon Differentiation of Mammary Epithelial Cells

Yu Han[1,3], **Lynn Sanford**[1,3], **David M. Simpson**[1,3], **Robin Dowell**[2,3], **Amy E. Palmer**[1,3]

[1]Department of Biochemistry, University of Colorado Boulder, Boulder CO 80303

[2]Department of Molecular, Cellular and Developmental Biology, University of Colorado Boulder, Boulder CO 80309

[3]BioFrontiers Institute, University of Colorado Boulder, Boulder CO 80303

Abstract

Zinc is the second most abundant transition metal in humans and an essential nutrient required for growth and development of newborns. During lactation, mammary epithelial cells differentiate into a secretory phenotype, uptake zinc from blood circulation, and export it into mother's milk. At the cellular level, many zinc-dependent cellular processes, such as transcription, metabolism of nutrients, and proliferation are involved in the differentiation of mammary epithelial cells. Using mouse mammary epithelial cells as a model system, we investigated the remodeling of zinc homeostasis during differentiation induced by treatment with the lactogenic hormones cortisol and prolactin. RNA-Seq at different stages of differentiation revealed changes in global gene expression, including genes encoding zinc-dependent proteins and regulators of zinc homeostasis. Increases in mRNA levels of three zinc homeostasis genes, *Slc39a14* (ZIP14) and metallothioneins (MTs) I and II were induced by cortisol but not by prolactin. The cortisol-induced increase was partially mediated by the nuclear glucocorticoid receptor signaling pathway. An increase in the cytosolic labile Zn^{2+} pool was also detected in lactating mammary cells, consistent with upregulation of MTs. We found that the zinc transporter ZIP14 was important for the expression of a major milk protein, whey acid protein (WAP), as knockdown of ZIP14 dramatically decreased WAP mRNA levels. In summary, our study demonstrated remodeling of zinc homeostasis upon differentiation of mammary epithelial cells resulting in changes in cytosolic Zn^{2+} and differential expression of zinc homeostasis genes, and these changes are important for establishing the lactation phenotype.

Graphical Abstract

*To whom correspondence should be addressed: Amy.palmer@colorado.edu, 303-492-1945, 3415 Colorado Ave., Boulder CO 80303.

Author contributions

Y.H. and A.P. designed the research and analyzed the results. Y.H. carried out the majority of the research. L.S. helped with RNA-Seq and enrichment analysis. D.S. carried out cloning for the promoter assay. R.D. assisted with RNA-Seq analysis and provided critical feedback. Y.H. and A.P. wrote the paper with edits from all authors.

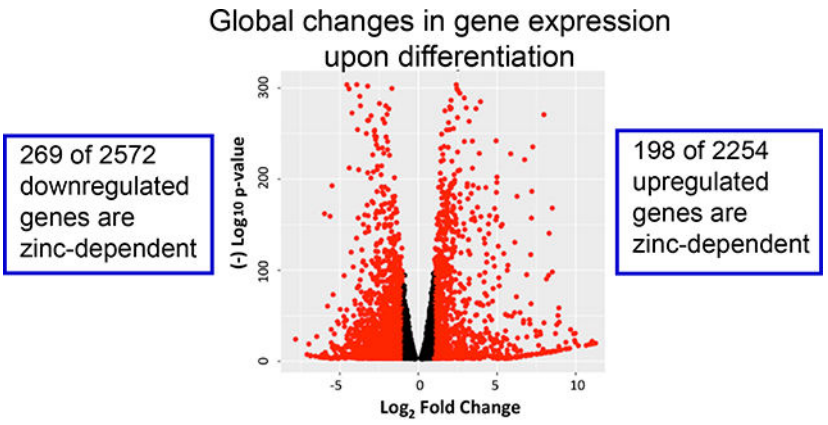

Introduction

Zinc (Zn^{2+}) is an essential trace element in humans and its importance is underscored by the discovery that up to 10% of the proteins encoded by the human genome are predicted to contain at least one zinc binding site[1]. Zinc-dependent proteins play critical roles in DNA synthesis, transcriptional regulation, and metabolic processes, and hence are important for many cellular functions[1,2]. Zinc homeostasis refers to the process by which Zn^{2+} is acquired, distributed and maintained in tissues and cells, and homeostasis is dynamically regulated to meet the specific need for Zn^{2+} by proteins under different biological conditions. Many of the key players in mammalian Zn^{2+} homeostasis have been identified. These players include transporters (genes *Slc39a1–14* encode ZIP proteins and genes *Slc30a1–10* encode ZnT proteins) that are responsible for the import and export of Zn^{2+} across the plasma membrane and intracellular organelle membranes, buffers such as metallothioneins (MTs) that have been suggested to regulate labile Zn^{2+} levels in cells, and transcription factors, such as MTF-1, that regulate expression of MTs and Zn^{2+} exporters[2,3]. While we know many of the proteins involved in mammalian Zn^{2+} homeostasis, we still lack a comprehensive picture of how cells sense and regulate Zn^{2+} availability and how the cooperative action of Zn^{2+} transporters, buffers and transcriptional regulators is coordinated. For example, while MTF-1 regulates expression of MTs, ZnT1, and ZnT2, how the expression of other zinc homeostasis proteins is controlled in order for cells to respond to shifting Zn^{2+} needs is unclear.

Mammary epithelial cells (MECs) are the basic units of milk production and undergo differentiation from a proliferative to a secretory phenotype during lactation in order to secrete large amounts of zinc (1–3 mg/day) as well as other nutrients into mother's milk[4]. Many of the changes in cell physiology that accompany differentiation are zinc-dependent. For example, transcriptional remodeling requires zinc-dependent transcription factors, proliferation is a zinc-dependent process[5], and matrix metalloproteinases (MMPs) are zinc-dependent enzymes that are secreted by MECs to remodel the architecture of the mammary gland and whose expression levels are regulated in a temporal fashion throughout lactation[6]. Previous work has revealed that the level of total Zn^{2+} and the expression level of many Zn^{2+} transporters is altered in the mouse lactating mammary gland during lactation [7,8].

However, a comprehensive global analysis of the changes in Zn^{2+} homeostasis and Zn^{2+}-dependent molecular processes over the course of differentiation has not been carried out.

In this study, we used HC11 cells as a model system to define changes in Zn^{2+} homeostasis in lactating MECs. HC11 mouse mammary epithelial cells can be differentiated into a secretory phenotype upon treatment of lactogenic hormones (prolactin and cortisol) and have been widely used to recapitulate molecular and cellular processes in lactating MECs[9,10]. In order to provide a comprehensive picture of how Zn^{2+} homeostasis and Zn^{2+}-dependent processes change over the course of differentiation, we performed next-generation RNA sequencing of HC11 cells to examine global changes in gene expression. Our analysis identified that the majority of zinc homeostasis genes were differentially regulated at a late stage of cell differentiation. Secondly, we quantified the labile cytosolic Zn^{2+} pool over the course of HC11 differentiation using genetically-encoded Zn^{2+} FRET sensors and discovered a 50% increase in cytosolic Zn^{2+} in differentiated cells. Lastly, we identified that a cortisol-induced transporter, ZIP14, contributes to the increase of cytosolic Zn^{2+} level and is important for the mRNA expression of whey acid protein, a major milk protein, suggesting an important association between zinc homeostasis and milk production.

Methods

Chemicals and reagents

Tris (2-pyridylmethyl) amine (TPA) was purchased from Sigma-Aldrich (catalog number 723134) and diluted with dimethyl sulfoxide (DMSO) to prepare 20 mM stock solutions. Stock solutions (5 mM) of 2-mercaptopyridine N-oxide (pyrithione, Sigma-Aldrich, catalog number 188549) were prepared in DMSO. Nuclear staining was achieved with NucBlue Live ReadyProbes Reagent (Thermo Fisher, catalog number R37605) for live cells or Hoechst 33258 (Sigma-Aldrich 861405) for fixed cells. An aqueous $ZnCl_2$ solution (1 mM) was diluted in phosphate-free HEPES-buffered Hanks' balanced salt solution (HHBSS, 1.26 mM $CaCl_2$, 1.1 mM $MgCl_2$, 5.36 mM KCl, 137 mM NaCl, 16.65 mM D-glucose, and 30 mM HEPES, pH 7.4) to make a 200 μM $ZnCl_2$ stock solution. An insulin stock solution (4 mg/mL) was purchased from Life Technologies (catalog number 12585014). Human recombinant epidermal growth factor (EGF, VWR 47743–566) was prepared as a 10 μg/mL stock solution in water. Prolactin (Sigma-Aldrich L6520) was prepared as a 5 mg/mL stock solution in water. A stock solution (138 μM) of hydrocortisone (Sigma-Aldrich H0888) in absolute ethanol was also prepared. Trace-metal grade nitric acid (65% −70%) was purchased from FLUKA (02650). For ICP-MS experiments, Y standard solution (10 ppm) was purchased from Inorganic Ventures (IV-stock-53–125 mL), Ga standard solution (1000 ppm) was purchased from Inorganic Ventures (ICP - CGGA1–125ML) and Zn standard solution (1000 ppm) was purchased from VWR (Cat. No. RCMSZN1KN-100).

Cell culture

HC11 cells were grown and maintained in proliferation (P) medium (RPMI supplemented with 10% (v/v) fetal bovine serum (FBS), 1% (v/v) penicillin/streptomycin (pen/strep), 10 ng/mL EGF and 5 μg/mL insulin). To induce cell differentiation, 4×10^5 cells were plated in a 35-mm dish (or 1×10^6 cells in a 10-cm dish) in proliferation medium. Cells reached

confluency after 3 days. Cells were maintained in resting (R) medium containing RPMI, 2% FBS (v/v), 1% pen/strep (v/v), 5 μg/mL insulin for one additional day, then treated with differentiation (D) medium containing 2% FBS, 1% pen/strep, 5 μg/mL insulin, 5 μg/mL prolactin, and 1 μM hydrocortisone for up to 6 days. Differentiation medium was changed every 2 days. In P media the cells doubled every 36 hr. Proliferation was generally inhibited when the media was switched to R. The differentiated cells exhibited different morphology compared to cells treated with R for the same time period. Differentiated cells were clumpier and more clustered, as observed in previous studies[11,12]. Samples were collected at the following time points for downstream analysis: P day 2 (cells growing in proliferation medium for 2 days since plated), R day 1 or day 6 (cells growing in resting medium for 24 hr or 7 days), D 12 hr, 24 hr, day 3 and day 6 (cells incubated in differentiation medium for the corresponding time).

Lentiviral transduction

HEK293T cells were maintained in RPMI medium supplemented with 10% FBS and transfected with lentiviral packaging plasmids and viral expression plasmids (which encode the promoter reporter constructs or ZIP14 shRNAs) using the TransIT-LT1 (Mirus Bio) reagent following the manufacturer's instruction. The packaging plasmids were a gift from Dr. Hubert Yin (University of Colorado, Boulder), containing pRev, which encodes the reverse transcriptase protein (Rev), pMDL, which encodes the Gag and Pol proteins, and pVSV-G, which encodes the Env protein. Medium was changed at 24 hr after transfection. By day 3 after transfection, medium was filtered using a 0.22 μm filter and the virus-containing medium supplemented with 8 μg/mL of polybrene was added to HC11 cells. After 3 days, puromycin (3 μg/mL) was added to HC11 cells to select for cells with stable expression of exogenous genes. Cells that survived puromycin selection were recovered in proliferation medium and stored in liquid nitrogen for future use.

shRNA knockdown (KD) of ZIP14

Four individual ZIP14-targeted shRNA constructs were stably expressed in HC11 cells using lentiviral transduction (Genecopoeia, Cat. No. LVRU6MP-MSH038111–31,32,33,34). Transduced cells were selected by puromycin and expression of a red fluorescence protein (mCherry) marker using flow cytometry. The efficiency of ZIP14 KD was examined by RT-qPCR.

RT-PCR and RT-qPCR

HC11 cells were trypsinized and harvested. Cell pellets were stored at −80 °C after flash freezing in liquid nitrogen until use. RNA purification, DNA removal and reverse transcription were performed following manufacturer's protocols. Specifically, RNA was purified with the RNeasy Mini Kit (QIAGEN, Cat. No. 74106); DNA was removed by DNaseI treatment (Thermo Scientific Cat. No. EN0525); RNA was reverse transcribed to cDNA using oligodT primers (Invitrogen, Cat. No. 18418012) and the Omniscript RT Kit (QIAGEN, Cat. No. 205113). RNase inhibitor (RNaseOUT Recombinant Ribonuclease Inhibitor, Invitrogen, Cat. No. 10777019) was supplemented in all reaction mixtures to inhibit RNA degradation. The synthesized first-strand cDNAs were then used as templates in the RT-PCR or RT-qPCR reactions. RT-PCR and RT-qPCR reactions were performed using

Phusion DNA polymerase (NEB, Cat. No. M0530S) and SYBRTM Green PCR Master Mix (Applied Biosystems, Cat. No. 4367659), respectively, following manufacturer's protocols. Quantitative analysis of relative expression of target genes normalized to reference genes using qPCR data was performed with the Pfaffl method as previously described[13]. Detailed information including RT-qPCR protocols, primer sequences and quantification method (standard curve, efficiency) are provided in Supporting Information.

Western blotting

HC11 cell pellets were resuspended in cold RIPA buffer supplemented with 1 mM dithiothreitol (DTT) and a protease inhibitor cocktail (one tablet per 10 mL, cOmplete, Roche, Cat. No. 04693159001). The mixture was incubated at 4 °C for 30 minutes on a rotator, followed by centrifugation at 14,000 rpm at 4 °C for 30 min. The pellet containing cell debris and nuclei was discarded. The protein concentration in the supernatant fraction was measured by the BCA assay (PierceTM BCA Protein Assay Kit, Thermo ScientificTM, Cat. No. 23225). 15 μg of protein was mixed with 5x SDS-loading dye and denatured at 95 °C for 5 min (CSN2 immunoblot). The protein mixture was separated in 10% (w/v) acrylamide gels for SDS-PAGE and then transferred to PVDF membranes at 80 V for 1 hr. The membrane was blocked in 5% (w/v) non-fat milk in 1x TBS-T (1x TBS with 0.1 % (v/v) Tween20, pH 7.4) at room temperature for 1 hr. The membrane was incubated with the primary antibody in blocking buffer overnight at 4 °C. The next day, the membrane was washed with 1x TBS-T for 30 min (10 min x 3 washes) and incubated in secondary antibody in blocking buffer at room temperature for 1 hr. Membrane was washed with 1x TBS-T for 30 min (10 min x 3 washes) again. Blots were developed with the Amersham ECL Prime Western Blotting Detection Reagent (GE Healthcare Life Sciences, Cat. No. RNP2232) and imaged on an ImageQuant LAS4000 imaging system (GE Healthcare Life Sciences). The antibodies used in immunoblotting were as follows: Beta-CSN2: the primary antibody was the goat anti-β-casein polyclonal antibody (Santa Cruz Biotechnology, SC-17971), 1:4,000 dilution; secondary antibody was donkey anti-goat IgG (H+L) secondary antibody (HRP) (Novus Biologicals, Cat. No. NB7357), 1:40,000 dilution. ACTB: the primary antibody was mouse anti-β-actin antibody (Sigma, A2228), 1:10,000 dilution; secondary antibody was goat anti-mouse IgG (H+L) secondary antibody (HRP) (Novus Biologicals, Cat. No. NB7539), 1:20,000 dilution.

Immunofluorescence

For immunofluorescence detection of CSN2, HC11 cells were grown on glass coverslips and induced to differentiate. Samples were collected at the following time points: P day 2, R day 1, D 12 hr, 24 hr, day 3 and day 6. Cells were washed with phosphate-buffered saline (PBS) three times and then fixed in 4% paraformaldehyde (PFA) in PBS for 45 min in the dark at room temperature. Cells were washed with PBS three times, followed by incubation with 20 mM NH_4Cl in PBS for 5 min at room temperature. Samples were stored in PBS at 4 °C until use. For permeabilization of the cell membrane, cells were incubated with 0.2% Triton X-100 in PBS solution for 15 min at room temperature, followed by washing 3x with PBS and blocking in 5% bovine serum albumin (BSA) for 45 min. Cells were washed with PBS three times and then incubated with primary antibody (goat anti-β-casein polyclonal antibody, Santa Cruz Biotechnology, SC-17971, 1:10 dilution) at room temperature for one

hr. Cells were washed with PBS three times and then incubated with secondary antibody (donkey anti-goat IgG-FITC, Santa Cruz Biotechnology, SC-2024, 1:20 dilution) at room temperature for one hr. Cells were then washed with PBS three times. To stain nuclei, cells were incubated with 1 mg/mL Hoechst 33258 in H_2O for 30 seconds at room temperature and then washed with PBS three times prior to mounting on glass slides.

CSN2 immunofluorescence images were acquired on a Nikon A1R laser scanning confocal microscope equipped with the Nikon Elements software platform, Ti-E Perfect Focus system with a Ti Z drive, using a 100x oil objective (NA 1.45) and the following channels: CSN2 (green) (488 nm laser line, PMT gain: 45 or 110, pinhole size: 1 or 4 AU, emission filter: 525/50 nm); Hoechst 33258 (blue) (405 nm laser line, PMT gain: 80 or 95, pinhole size: 1 AU, emission filter: 450/50 nm).

RNA-Seq

To prepare samples for RNA-Seq, three biological replicates of HC11 cells were trypsinized and harvested. Cell pellets were stored at −80 °C after flash freezing until use. RNA was extracted with the RNeasy Mini Kit (QIAGEN, Cat. No. 74106). DNA was removed by DNaseI treatment (Thermo Scientific Cat. No. EN0525). RNA samples were then submitted to the BioFrontiers Next-Gen Sequencing Core Facility at University of Colorado for library construction and sequencing. Specifically, libraries were prepared using the NEXTflex Rapid Illumina Directional RNA-Seq Library Prep Kit with polyA enrichment (Bioo Scientific). Sequencing was performed on the NextSeq platform using paired-end reads (High Output, 2 × 75). After sequencing, read quality was assessed using FastQC (version 0.11.2). Illumina adapters were trimmed using Trimmomatic 0.32 in paired-end mode (HEADCROP:10). Reads were then mapped to the mm10 genome (downloaded from NCBI) using Tophat 2.0.6 with the options {b2-very-sensitive -p 12 -r 240 --mate-std-dev 105 –library-type fr-secondstrand} [14]. Mapped reads were counted using HTSeq (version 0.6.1)[15] with the options {-f -r -s -m intersection-strict}. Differential expression of genes was analyzed using the R(version 3.4.1) package DESeq2 (version 1.16.1)[16]. The expression levels of Zn^{2+} homeostasis genes were represented as transcripts per million mapped reads (TPM) using the following equation: $\mathrm{TPM} = 10^6 \times A \times \frac{1}{\sum(A)}$, A = (total reads mapped)/(gene length in kilo bp). Gene ontology (GO)-derived functional annotations were analyzed using DAVID 6.8 with GOTERM_BP_DIRECT (BP: biological processes), GOTERM_MF_DIRECT (MF: Molecular Function) and KEGG Pathways. Enrichment of biological processes and pathways was ranked based on the adjusted p-value (Benjamini score) associated with each annotation term, with a lower score indicating more significant enrichment.

All raw next-generation sequencing data files and processed data files used to draw conclusions are available at the Gene Expression Omnibus.

Inductively coupled plasma mass spectrometry (ICP-MS)

All ICP-MS samples were spiked with known amounts of two internal standard elements, Yttrium (Y) and Gallium (Ga), to correct technical or human errors. The ion counts of zinc (Zn) in each sample measured by ICP-MS were corrected by the ratio of measured Y or Ga

(ppb) to the known amount of Y or Ga (ppb). The Zn ion counts were then converted to parts per billion (ppb) using a Zn standard curve. The Zn ppb signal was normalized to total cell number to compare Zn in different samples. To prepare the HC11 cells for ICP-MS, 10×10^6 cells were trypsinized and harvested in 15 mL metal-free conical tubes (VWR, 89049–172) and then cell pellets were dried at 50 °C in a fume hood overnight. The next day, 200 μL of Trace-metal grade 65% Nitric Acid (FLUKA, 02650) was added to cell pellets and the mixture was heated in boiling water for 30 minutes. After the samples cooled down to room temperature, the nitric acid concentration in samples was corrected to 2 % using chelex-treated Milli-Q water. 5 ppb of Y and 5 ppb of Ga were added to each sample as internal standard elements. Samples were submitted for ICP-MS analysis to the LEGS Lab at CU Boulder. Zn (ppb) was converted to the concentration ([Zn]) of Zn per cell. Detailed protocols and data analysis are presented in Supporting Information.

Measurement of labile cytosolic Zn^{2+} using NES-ZapCV2

An HC11 cell line stably expressing the cytosolic Zn^{2+} sensor NES-ZapCV2[17] was generated using the PiggyBac transposase system (System Biosciences) following the manufacturer's instruction. Fluorescence imaging was performed on a Nikon Ti-E wide-field fluorescence microscope equipped with Nikon elements software, an iXon3 EMCCD camera (Andor), mercury arc lamp, and FRET (434/16 excitation, 458 dichroic, 535/20 emission), CFP (434/16 excitation, 458 dichroic, 470/24 emission), and YFP (495/10 excitation, 515 dichroic, 535/20 emission) filter sets. To perform a titration experiment, fluorescence intensities of FRET, CFP and YFP channels of a randomly selected cytoplasmic region (cytosol) and a region without cells (background) were recorded every 40 seconds for ~ 3 min in the resting state. The FRET ratio was calculated as $(FRET_{cytosol} - FRET_{background}) / (CFP_{cytosol} - CFP_{background})$ and all ratios were then averaged to acquire the resting ratio (R). Cells were then treated with 150 μM TPA (Zn^{2+} chelator) for an extended time (~ 20 min) to ensure that FRET R decreased and stabilized. The minimum ratio, R_{min}, was acquired by averaging ratios of the last 3 time points of TPA treatment. After cells were washed twice with phosphate-free HHBSS buffer, a mixture of pyrithione (a Zn^{2+} ionophore, final concentration 0.75 μM) and $ZnCl_2$ (final concentration 20 μM) was added to cells until the FRET ratio increased and reached a plateau. The maximum ratio, R_{max}, was calculated by taking the mean of all ratios measured in the plateau phase. The labile Zn^{2+} concentration was calculated using this equation: $[Zn^{2+}] = K_d \times [(R-R_{min}) / (R_{max}-R)]^{1/n}$. For the NES-ZapCV2 cytosolic sensor, the K_d = 2.3 nM and the Hill Coefficient (n) = 0.532 [17]. Alternatively, the labile Zn^{2+} concentration can be represented as the fractional saturation (FS) of the sensor, which was defined as $FS = (R - R_{min}) / (R_{max} - R_{min})$. Cells with a dynamic range (R_{max} / R_{min}) in the range of 1.5 – 2.5 were selected for analysis.

Promoter reporter assay

The promoter reporter assay designed to test promoter activity in response to hormone treatment was performed using the Secrete-Pair Dual Luminescence Assay Kit (GeneCopoeia) following the manufacturer's instructions. The CSN2 promoter was amplified from the HC11 cell genome using the NucleoSpin BloodXL kit (MACHEREY-NAGEL, ref 740950.50) and inserted into multiple cloning site 1 (MCS1) of the pEZX-

LvGA01 vector (GeneCopoeiaTM, catalog No. ZX107) 5' upstream of the Gaussia Luciferase (GLuc) ORF. The 983-bp promoter sequence includes a ~900 bp fragment upstream of the transcription start site (TSS) and a ~100 bp fragment downstream of the TSS. The TSS position was acquired from the Eukaryotic Promoter Database (EPD). Primers sequences are: Csn_Fwd 5' TCTGATGAATTCTCTGTAATTACTATTATTAAAAAGATTAATGTTTGTTAAG 3'; Csn_Rev 5' ATCAGAACCGGTCTAGTATGCATTTGAAATAATGAAAATGATATTTC. This vector also constitutively expresses an internal control reporter, SEAP (secreted alkaline phosphatase). Both GLuc and SEAP can be secreted into cell media upon being synthesized. The promoter activity is reported using the ratio of GLuc signal to the SEAP signal. HC11 cell lines stably expressing promoter constructs were generated using lentiviral transduction and selected for successful transduction by puromycin. To determine the promoter activity in response to lactogenic hormone treatment, 4×10^5 HC11 stable cells were plated in a 35 mm dish in the proliferation media (2 mL) for 3 days and then cultured in the resting media (2 mL) for one more day. Cells were then treated with the lactogenic hormones for 6 days with fresh media replaced every 2 days. For luciferase analysis, 200 μL of media was collected at 4, 18, 24 hr, day2, 3, 4, 5 and 6 post hormone treatment. 200 μL of fresh media was added back to cell culture to compensate for the volume change after media collection. All samples were frozen at −20 °C. The GLuc and SEAP catalyzed luminescence reactions were performed using the Secrete-Pair ™ Dual Luminescence Assay Kit (GeneCopoeia) following the manufacturer's instructions. Luminescence was recorded using a BioTek Synergy H1 hybrid plate reader (gain: 200; integration time: 3 s). 2 biological replicates were utilized at each time point and 3 technical replicates were measured for each biological replicate.

Results

Characterization of HC11 cell differentiation

The murine mammary epithelial cell line HC11 has been widely used as an *in vitro* model system to investigate mammary cell differentiation[18–20]. The cell line was isolated from the COMMA-1D mammary epithelial cell line[9] which was established from the mammary tissue of BALB/c mice in the middle of pregnancy[21], and the expression of several milk genes can be induced by a combination of lactogenic hormones (prolactin and cortisol) without the requirement of any matrix protein[9,10]. HC11 cells were differentiated using a previously established protocol[9,22] (Figure 1A). The progression of differentiation was characterized by measuring the expression of two lactation markers casein (CSN2) and whey acid protein (WAP) in samples from the proliferation state (P day2), resting state (R day1) and upon treatment with prolactin and cortisol, representing the differentiation state (D 12 hr, day1, day3 and day6). *Csn2* and *Wap* mRNA were not detected until 3 days after hormone treatment and the mRNA levels of both genes further increased at day 6 after treatment (Figure 1B). CSN2 protein levels, as detected by Western blotting, appear at 3 days after treatment and increase further 6 days after treatment, paralleling the mRNA signature (Figure 1C). To examine differentiation at the single cell level, immunofluorescence of CSN2 protein expression was performed over the course of differentiation. The total number of cells and number of cells that stained positively for

CSN2 expression were manually counted and the percentage of cells with detectable CSN2 expression was quantified. CSN2 expression was essentially undetectable in P day2 (0.00%) and R day1 samples (0.08%) (Figure 1D). After hormone treatment, the percentage of cells with detectable CSN2 was as follows: D 12 hr (0.74%), day 1 (0.68%) and day 3 (13.4%) samples. By day 6 after hormone treatment, CSN2 expression was detected in almost every cell (95.5%). Although it took 3 days of hormone treatment to detect the steady-state mRNA and protein level of lactation markers, using a luciferase promoter assay, gene transcription from the CSN2 promoter was initiated by 18 hr of hormone treatment and transcriptional activity continued to increase from day 1 to day 6 post lactogenic hormone treatment (Figure 1E).

Changes in global gene expression at 24 hr and 6 days post hormone treatment

To define how treatment with lactogenic hormones remodeled global gene expression of mammary epithelial cells, next-generation RNA sequencing (RNA-Seq) was performed on R day1 (control), D day1 (early stage differentiation) and D day6 (later stage differentiation) samples, with 3 biological replicates for each condition. The expression of genes in D day1 and D day6 samples relative to R day1 samples was analyzed pairwise using DESeq2, revealing that 1909 and 8161 genes were differentially expressed at D day1 and D day6 compared to R day1, respectively ($p_{adj} < 0.001$). Figure 2A shows volcano plots depicting statistical significance vs. fold change of the differentially expressed genes. The genes that were differentially expressed by more than 2-fold are highlighted in red, with 1132 genes at day 1 and 2943 genes at day 6 post hormone treatment, which account for 4.5% or 11.7% of 25059 total mouse genes.

To gain insight into the biological functions and pathways that were altered upon differentiation, gene ontology (GO)-derived functional annotations of the downregulated and upregulated genes at day 1 and day 6 (fold change > 2, $p_{adj} < 0.001$) post-hormone treatment were analyzed using DAVID 6.8 with GOTERM_BP_DIRECT (BP: biological processes) and KEGG Pathways (Figure 2B, Supp Info RNAseq). Cell cycle and cell division processes were significantly downregulated at day 1, and further downregulated at day 6 post-hormone treatment, consistent with the shift away from a proliferation phenotype. The major biological processes and pathways that were upregulated in the early stage of differentiation D day1 were cell adhesion, ECM-receptor interaction and protein digestion and absorption. By D day6, pathways involved in cell metabolism and secretion were upregulated, such as protein digestion and absorption, ion transport and absorption, and lysosome. Overall, RNA-Seq revealed that lactogenic hormone treatment temporally altered the activities of different biological processes in mammary epithelial cells. A full list of regulated GO and KEGG terms is included in the Supporting Information RNAseq file.

Zinc-dependent genes are differentially expressed upon differentiation

To explore how the expression of zinc-regulatory and zinc-dependent genes were modulated by lactogenic hormone treatment, the differentially expressed genes at day 1 and day 6 post hormone treatment (fold change > 1.5, $p_{adj} < 0.001$) were analyzed using DAVID 6.8 with UniProt (UP)_Keywords. According to the definition of the keyword “Ligand” (KW9993) in the Uniprot database, the UP_Keyword “Zinc” (KW0862, which is in the “Ligand”

category) was assigned to genes when the translated gene products (i.e. proteins) bind, are associated with, or have activity that is dependent on zinc. In D day1 samples, 96 out of 942 (10.2%) downregulated genes and 46 out of 761 (6.0%) upregulated genes (fold change >1.5) were annotated with the keyword “Zinc”. In D day6 samples, 269 out of 2572 (10.4%) downregulated genes and 198 out of 2254 (8.8%) upregulated genes (fold change >1.5) were annotated with “Zinc” (Figure 3A). The differentially expressed “Zinc”-annotated genes at D day6 were then sorted based on fold change or p_{adj}. Interestingly, two zinc transporters, *Slc39a8* (ZIP8) and *Slc39a14* (ZIP14), were reported among the top 10 genes with highest fold change or lowest p_{adj} respectively (Table S6).

To further examine functional categories of differentially expressed zinc-dependent genes, the functional annotations of downregulated and upregulated genes in D day1 and D day6 samples (fold change > 1.5, $p < 0.001$) were analyzed using GOTERM_BP and GOTERM_MF_DIRECT (MF: Molecular Function), as described previously (Figure 3, Supporting Information_RNAseq). GO_MF terms “metal ion binding” and “zinc ion binding” are excluded, as all of the zinc-dependent genes bind zinc/metal and therefore those terms are enriched in each comparison. Upon hormone treatment, 15 zinc-dependent biological and molecular processes are enriched at D day1, including intracellular signal transduction, DNA/protein binding, regulation of gene transcription, and metabolic enzyme activities (Figure 3A, 3B). At D day6, 55 zinc-dependent processes are enriched, including cell signal transduction, transcription, protein ubiquitination and metabolic enzyme activities. Interestingly, GO enrichment analysis demonstrated that “zinc II ion transport” (GO_BP), “cellular zinc ion homeostasis” (GO_BP) and “Zinc ion transmembrane transporter activity” (GO_MF) are upregulated at day 6 post hormone treatment, indicating that zinc transport and distribution may also be altered upon hormone treatment. A full list of regulated GO and KEGG terms is included in the Supporting Information RNAseq file.

Zinc homeostasis genes are differentially expressed upon differentiation

Zn^{2+} homeostasis is regulated by Zn^{2+} transporters, Zn^{2+} buffering protein metallothioneins (MTs) and the metal-responsive transcription factor 1 (MTF1)[23]. To understand how cell differentiation regulates zinc homeostasis, we used our RNA-Seq data to analyze how known zinc regulatory genes change upon differentiation. Because many Zn^{2+} transporters are expressed at low levels, we first examined the average transcripts per million mapped reads (TPM) for each Zn^{2+} regulatory gene (Figure 4A). Genes with TPM < 1 were not included in differential expression analysis because the expression level was deemed too low to be reliable. Twenty Zn^{2+} homeostasis genes with TPM > 1 were detected in all conditions and analyzed for differential expression using DESeq2. Two genes, ZIP4 and ZIP11, were differentially regulated at D day1 (Figure 4B). After 6 days of hormone treatment, 14 genes were differentially expressed. Among these, 3 genes encodeding ZIP transporters were downregulated, while 11 genes encoding 5 ZIPs, 3 ZnTs, 2 MTs and MTF1 were upregulated. These results demonstrate that expression of Zn^{2+} homeostasis genes is remodeled upon treatment with lactogenic hormones, consistent with previous studies using RT-qPCR[8], and reveal that Zn^{2+} homeostasis is more dramatically altered at a late stage of cell differentiation. For downstream analysis of how hormones affect zinc homeostasis genes, ZIP14, MT1 and MT2 were chosen as targets because of their relatively high

expression level and fold change in D day6 samples compared to that observed in resting cells.

Cortisol increases the steady-state level of ZIP14, MT1 and MT2 mRNAs

Two lactogenic hormones, prolactin and cortisol, were used to initiate HC11 cell differentiation. These two hormones function through different signaling pathways and we wanted to determine which was most influential in remodeling Zn^{2+} homeostasis. To examine the role of each hormone in regulating the mRNA levels of Zn^{2+} homeostasis genes, HC11 cells were cultured in proliferation media or resting media as in the differentiation protocol and then treated with prolactin (Prl), cortisol (Cor), or both hormones (Prl + Cor) for 6 days. Cells were collected at day 1 post treatment with resting media (R day1), and day 6 post treatment with hormone(s) (Prl day6, Cor day6 and Prl+Cor day6). To eliminate the possibility that the higher levels of mRNA for Zn^{2+} homeostasis genes resulted from extended culturing, we also collected cells that continued to grow in the resting media for another 6 days (R day6). Using RT-qPCR, expression of ZIP14, MT1 or MT2 was analyzed and normalized to two reference genes: beta actin (ACTB) and ribosomal protein S9 (RPS9). CSN2 was used as a positive control because its mRNA expression was strongly activated by the treatment of prolactin and cortisol, as shown previously[9]. Cortisol was the primary factor that increased the steady-state level of ZIP14, MT1 and MT2 mRNAs (Figure 5A). Prolactin treatment alone had no effect on the mRNA levels of ZIP14, MT1 and MT2. On the other hand, cortisol treatment alone (Cor day6) significantly increased the expression of ZIP14, MT1, and MT2 compared to their expression level in R day1, R day6 or P day6 samples. Finally, there was no significant difference in the mRNA levels of ZIP14, MT1 and MT2 between the cells treated with cortisol alone (Cor day6) and the cells treated with both hormones (Prl+Cor day6).

To examine whether cortisol affects the mRNA level of ZIP14, MT1 and MT2 via the canonical glucocorticoid receptor (GR) signaling pathway, HC11 cells were treated with a GR antagonist RU486 to competitively inhibit receptor binding with cortisol[24]. The optimal dosage of RU486 was determined by supplementing differentiation media with different amounts of RU486 and quantifying the mRNA of MT2 by RT-qPCR under each condition. MT2 was used as a positive control for cortisol dependence because previous work showed cortisol increased MT2 mRNA levels and RU486 abolished the effect[24]. Treatment with 100 nM RU486 significantly lowered the MT2 mRNA level compared to vehicle and 10 nM RU486 treatment ($p < 0.0001$), while there was no difference between 100 nM and 1 μM (Figure 5B). It was noteworthy that 100 nM RU486 did not reduce the mRNA level of MT2 to the basal level observed in the R day1 samples. To assess the effect of RU486 on the mRNA level of MT1 and ZIP14, HC11 cells were treated with the differentiation media supplemented with 100 nM RU486 for 6 days and the relative expression of ZIP14 and MT1 was determined using RT-qPCR. The steady-state ZIP14 mRNA level was lowered by RU486 treatment compared to the vehicle group, but it was still higher than that of basal level in the R day1 samples (Figure 5C). The effect of RU486 on MT1 mRNA level was inconclusive due to the variance of the results (Figure 5D). When normalized to RPS9, the MT1 mRNA level in the vehicle-treated and RU486-treated samples was significantly different. However, when normalized to ACTB, the difference in MT1 mRNA level between

the vehicle-treated and the RU486-treated groups was not statistically significant ($p = 0.0499$). Overall, these data show that a competitive GR inhibitor significantly abrogated the cortisol-induced increase in expression of ZIP14 and MT1, indicating that cortisol induces these genes at least partially via the nuclear GR signaling pathway.

Total Zn^{2+} doesn't change, but labile cytosolic Zn^{2+} increases over the progression of cell differentiation

Our observation that MTF1, MTs, and Zn^{2+} transporters are differentially expressed at a later stage of cell differentiation (day 6 after hormone treatment) led us to hypothesize that total or cytosolic labile Zn^{2+} might be altered. To determine total cellular Zn^{2+} over the course of differentiation, HC11 cells were treated with lactogenic hormones and Zn^{2+} was measured at different time points using ICP-MS, an elemental analysis technique that measures total metal in a bulk sample. We observed that total Zn^{2+} did not change over the progression of cell differentiation (Figure 6A). Labile Zn^{2+} in the cytosol was measured using NES-ZapCV2, a genetically-encoded Zn^{2+} FRET-based ratiometric sensor that localizes to the cytosol[17]. To quantify cytosolic Zn^{2+}, an in situ calibration was performed to acquire the resting FRET ratio (R), the minimum ratio (R_{min}) after treatment with the Zn^{2+} chelator TPA, and the maximum ratio (R_{max}) after treatment with the ionophore pyrithione and Zn^{2+} (Figure 6B). Statistical analysis revealed that cytosolic Zn^{2+} did not change at 12 or 24 hr post hormone treatment, but an increase in Zn^{2+} was detected in the D day3 samples compared to the resting state R day1 (R day1, 140 ± 30 pM; D day3, 170 ± 35 pM, $p < 0.0005$), with a further increase at day 6 post hormone treatment (D day6, 210 ± 60 pM, $p < 0.0001$ vs. R day1 or D day3). Combined with the result that the mRNA and protein expression of two differentiation markers (CSN2 and WAP) increased on day 3 of hormone treatment (Figure 1), our data suggest that higher cytosolic Zn^{2+} is positively associated with the progression of cell differentiation.

ZIP14 contributes to increased cytosolic Zn^{2+} and upregulation of WAP at day 6 post hormone treatment

Cytosolic labile Zn^{2+} is balanced between influx (regulated by ZIPs), efflux (regulated by ZnTs), and buffering (regulated largely by MTs) to stay at an optimal level. What defines the set-point of labile Zn^{2+} in cells is not well understood, but Zn^{2+} transporters have been shown to alter Zn^{2+} in different cellular compartments[24–27]. We wanted to perturb the changes in Zn^{2+} homeostasis upon differentiation in order to examine how Zn^{2+} might impact the differentiation phenotype. While there were changes in multiple transporters (both increases and decreases) upon differentiation, the 5-fold increase in ZIP14 expression was intriguing because of the overall high expression level of this trasporter. To explore how ZIP14 expression affected cytosolic Zn^{2+} levels, ZIP14 was knocked down using two shRNAs targeting different regions of ZIP14 mRNA and cytosolic Zn^{2+} was examined in D day6 cells using the NES-ZapCV2 sensor. HC11 cells stably expressing ZIP14 shRNA-1, ZIP14 shRNA-2 or scrambled control (SC) shRNA were treated with lactogenic hormones for 6 days and ZIP14 mRNA expression was quantified by RT-qPCR (Figure 7A). ShRNA-1 and −2 lowered the ZIP14 mRNA expression by 27% and 34%, respectively (ZIP14/ACTB in SC cells: 1.00 ± 0.11; shRNA-1 cells: 0.73 ± 0.07; shRNA-2 cells: 0.66 ± 0.07). As shown in Figure 7B, the cytosolic Zn^{2+} concentration was significantly lower in ZIP14 KD

cells compared to control cells. The lower concentration in shRNA-2 cells is consistent with the fact that shRNA-2 lowered ZIP14 mRNA level more than shRNA-1. Importantly, treatment with shRNA essentially abolished the increase in Zn^{2+} upon differentiation, providing a window to explore how Zn^{2+} and a key Zn^{2+} transporter could influence the differentiation phenotype.

To investigate the role of ZIP14 in mammary cell differentiation and lactation, the mRNA expression of differentiation markers CSN2 and WAP was measured in ZIP14-KD cells using RT-qPCR. HC11 cells stably expressing ZIP14 shRNA-1, ZIP14 shRNA-2 or scrambled control (SC) shRNA were treated with lactogenic hormones for 6 days. ZIP14-KD did not change the steady state CSN2 mRNA level (Figure 7C). However, WAP mRNA expression decreased significantly in ZIP14-KD cells, with a greater effect by shRNA-2 (Figure 7D). With WAP relative expression in SC cells normalized to 1.00, the WAP expression level was 0.41± 0.06 (WAP/ACTB) and 0.35 ± 0.07 (WAP/RPS9) in ZIP14 shRNA-1 KD cells, 0.13 ± 0.02 (WAP/ACTB) and 0.12 ± 0.02 (WAP/RPS9) in ZIP14 shRNA-4 KD cells. This result suggests that ZIP14 specifically, and Zn^{2+} homeostasis in general, plays an important role in the induction of WAP mRNA but not CSN2 mRNA in differentiated mammary cells. This finding is surprising because WAP and CSN2 are induced by the cooperative and synergistic action of prolactin-activated JAK-STAT signaling and cortisol-activated glucocorticoid receptor (GR) signaling. Despite the similarities, other researchers have reported differences in the underlying mechanism of transcription regulation of the two genes. For example, cortisol alone is able to effectively induce WAP transcription but has little effect on CSN2 expression, whereas prolactin alone was sufficient to induce CSN2 but not WAP transcription[28,29]. Additionally, a transcriptional factor, nuclear factor 1(NF1) was found to be essential in the transcriptional activation of WAP along with the cooperation with STAT5 and GR[30]. An intriguing study revealed that NF1 binds and activates MT1 in a Zn^{2+}-inducible and MTF-1 dependent manner, suggesting an important link between NF1 and zinc homeostasis[31]. How Zn^{2+} homeostasis affects WAP but not CSN2 transcription is unknown and requires further investigation.

Discussion

The HC11 cell line is a well-established model system to recapitulate systematic changes in molecular and cellular processes of mammary epithelial cells during lactation. Previous transcriptomic studies using microarray[32,33] and next generation RNA sequencing[34] demonstrated global changes in gene expression in HC11 cells upon lactogenic hormone treatment. However, these studies only examined HC11 cell differentiation at day 3 after lactogenic hormone (prolactin and cortisol) treatment and therefore were unable to distinguish the cellular and molecular changes occurring at an early versus late stage of cell differentiation. Our RNA-Seq analysis revealed that 1132 genes (~ 4.5% of the mouse genome) were differentially regulated at 24 hr after treatment, consistent with a global change at an early stage of cell differentiation. GO_BP enrichment and KEGG pathway analysis of these 1132 genes suggested two major suppressed cellular functions are mitosis/cell division and cell cycle. For example, Cdk1 (Cyclin-dependent kinase 1) is a central player in driving mammalian cell cycle through G2/M phase[35] and its expression was decreased by more than 3 fold at 24 hr ($p < 0.0001$). The major functional clusters that are

regulated by differentiation hormones include cell adhesion, ECM-receptor interaction, cell cycle and division, which could play important regulatory roles in the preparation for cell differentiation.

Not surprisingly, by D day6, a higher number of biological processes/pathways were affected, including downregulation of pathways such as cell division, cell replication and a few signaling pathways (e.g. p53 and PI3K-Akt signaling pathways), as well as upregulation of ion transport and absorption, Lysosome and metabolism (protein digestion and absorption). The majority of the above processes/pathways are strongly overlapping with published transcriptomic studies where cells underwent 3-day treatment[32–34]. Nonetheless, our analysis uniquely identified enrichment of Endoplasmic Reticulum (ER) unfolded protein response (UPR) pathway in upregulated genes at D day6. During lactation, mammary gland epithelial cells synthesize a large quantity of proteins, which leads to the accumulation of unfolded proteins in the ER. A few key UPR factors (e.g. XBP1 and ATF4) have been demonstrated to be upregulated in the lactating mammary gland[36,37]. Furthermore, knockdown of ATF4 or XBP1 in HC11 cells suppressed the gene expression of beta-casein and the lactogenic hormone receptor[38], suggesting an essential role of the UPR in HC11 cell differentiation. In our study, enrichment of the UPR pathway and higher expression of essential UPR factors (33-fold increase of XBP1, 6.7-fold increase of ATF4, 2.7-fold increase of ATF6 Supporting Information_RNAseq) are consistent with previous studies and suggests that the UPR is upregulated during the differentiation of HC11 cells.

Using RNA-Seq, we also discovered that the majority of zinc homeostasis genes (14 out of 20 detected) and 467 zinc-dependent genes were differentially regulated by D day6. A number of studies have interrogated the regulation of expression and functional roles of select zinc transporters (i.e. ZnT2, ZnT4 and ZIP3) in differentiated HC11 cells[39–42]. For example, the expression of ZnT2 was shown to be activated by prolactin, and ZnT2 was proposed to import Zn^{2+} into the secretory pathway in differentiated HC11 cells, suggesting a role for ZnT2 in Zn^{2+} secretion into the milk lumen[39,40]. Additionally, ZnT4 and ZnT5 have been shown to be functionally related with milk production. A ZnT4 nonsense-mutation in lethal milk mice resulted in low zinc concentration in milk, and pups exclusively fed with the lethal milk die even before weaning[43]. In addition, reduced mRNA expression of ZnT5 was identified in breastfeeding women producing zinc-deficient milk[44].The most comprehensive study examined the mRNA and protein levels of all Zn^{2+} transporters in lactating versus non-lactating mouse mammary glands, revealing a number of changes in Zn^{2+} homeostasis upon lactation[8]. However, this study profiled changes in the entire mammary gland, which contains multiple cell types[45], and it focused on a single time point, as opposed to monitoring changes over the course of differentiation. Still, these prior studies provide an important foundation for our study, by demonstrating significant changes in Zn^{2+} transporter expression during differentiation.

In addition to changes in Zn^{2+} transporters, changes in labile Zn^{2+} levels have been previously detected upon differentiation. Specifically, an accumulation of Zn^{2+} in lysosomes and vesicular bodies was detected using small-molecule fluorescent Zn^{2+} dyes in HC11 cells at 16–24 hr post hormone treatment[7,46], suggesting a redistribution of intracellular Zn^{2+} among organelles during lactation. Here, we found two Zn^{2+} homeostasis genes and 142

Zn^{2+}-dependent genes with altered expression at day 1, and 11 Zn^{2+} homeostasis genes and 467 Zn^{2+}-dependent genes by day 6, suggesting that Zn^{2+} homeostasis starts to be remodeled at day 1, but is not complete until later stages of differentiation.

In exploring what causes the expression changes in key zinc regulatory genes, we demonstrated that cortisol, but not prolactin, increased the mRNA levels of ZIP14, MT1 and MT2. At first glance this was surprising given that Zn^{2+} can interact with prolactin and induce aggregation[47,48]. However, careful consideration of the concentrations of Zn^{2+} and prolactin in our media conditions reveals that the concentration of prolactin in our media is very low (0.2 μM) and most of the Zn^{2+} in the media is complexed with serum albumin[49], which binds Zn^{2+} more tightly than prolactin[50,51]. Therefore, we speculate that the Zn^{2+}-prolactin interaction isn't relevant in our model system. The induction of ZIP14 and MT2 was at least partially mediated by the classical nuclear glucocorticoid receptor (GR) signaling pathway. However, treatment with GR-specific antagonist RU486 did not completely abolished the mRNA increase of ZIP14 and MT2 in differentiated cells compared to resting cells, suggesting that another signaling pathway may also play a role in induction of these genes. In addition to the nuclear GR signaling pathway, recent studies have shown that cortisol can also activate cell surface receptors[52–55] or crosstalk with other signaling pathways (e.g. JAK-STAT)[24,56] which may contribute to the induction of ZIP14 and MT2. Additionally, it has been reported that ER stress and UPR responses induce ZIP14 expression[57,58]. UPR factors ATF4 and ATF6 directly bind the ZIP14 promoter and induce ZIP14 transcription in human and mouse[57,59]. Therefore, it is plausible that ATF4 and ATF6 directly enhance the transcription of ZIP14 in mammary cells, though how cortisol and UPR are correlated is unknown.

Zn^{2+} is an important structural and/or functional cofactor for ~10% of human proteins[1]. Therefore, it is reasonable that cytosolic labile Zn^{2+} would increase to meet the structural or functional needs of the upregulated cytosol-localized zinc-dependent proteins during mammary cell differentiation. Among the list of upregulated zinc-dependent genes at D day6, we found genes which reportedly encode cytosolic proteins that play important or essential roles in cell differentiation or lactation, including the vitamin D receptor (VDR)[60], Peptidylglycine alpha-amidating monooxygenase (PAM)[61] and Tristetraprolin (TTP)[62–64], a zinc-finger mRNA-binding protein encoded by ZIP36. TTP is highly expressed in differentiated mammary cells and the lactating mammary gland[62,63]. The importance of TTP in mammary cell function is underscored by the observation that a knockout of TTP in mice led to mammary cell death and underweight pups[62]. The concurrent increase of cytosolic Zn^{2+} and expression of the cytosol-localized zinc-dependent proteins exemplifies a mechanism of how cells temporally remodel zinc homeostasis to regulate protein function under different biological processes.

Conclusion

In conclusion, we comprehensively examined zinc homeostasis regulation at multiple levels over the course of HC11 mammary epithelial cell differentiation. We detected differential expression of a majority of zinc transporters and an increase in cytosolic Zn^{2+}. We discovered that ZIP14 played a significant role in increasing cytosolic Zn^{2+} in differentiated

cells, and that Zip14 expression was important for WAP expression and may play important biological roles in mammary epithelial cells differentiation or lactation.

Supplementary Material

Refer to Web version on PubMed Central for supplementary material.

Acknowledgements

We would like to acknowledge the following sources of financial support: NIH R01 GM105997 and Director's Pioneer Award DP1 GM114863 (to A.E.P), a Signaling and Cell Cycle Training Grant to L.S. (T32 GM008759), and a traineeship in the IQ Biology program of the BioFrontiers Institute to L.S. (NSF IGERT 1144807). We would like to acknowledge the University of Colorado BioFrontiers Institute Next-Gen Sequencing Core Facility, which performed the Illumina sequencing and library construction, the BioFrontiers Computing Core and BioFrontiers IT for providing High Performance Computing resources, and the University of Colorado Biochemistry Cell Culture Core Facility for providing resources for cell culturing. We also would like to thank Dr. Mary Allen (University of Colorado Boulder, BioFrontiers Institute) for helpful discussions and training in RNA-Seq analysis.

References

1. Andreini C, Banci L, Bertini I and Rosato A, Counting the Zinc-Proteins Encoded in the Human Genome, J. Proteome Res, 2006, 5, 196–201. [PubMed: 16396512]
2. Kambe T, Tsuji T, Hashimoto A and Itsumura N, The Physiological, Biochemical, and Molecular Roles of Zinc Transporters in Zinc Homeostasis and Metabolism, Physiological Reviews, 2015, 95, 749–784. [PubMed: 26084690]
3. Colvin RA, Holmes WR, Fontaine CPand Maret W, Cytosolic Zinc Buffering and Muffling: Their Role in Intracellular Zinc Homeostasis, Metallomics, 2010, 2, 306–317. [PubMed: 21069178]
4. Picciano MF and Guthrie HA, Copper, Iron, and Zinc Contents of Mature Human Milk, Am J Clin Nutr, 1976, 29, 242–254. [PubMed: 943927]
5. Beyersmann D and Haase H, Functions of Zinc in Signaling, Proliferation and Differentiation of Mammalian Cells, Biometals, 2001, 14, 331–341. [PubMed: 11831463]
6. Kelleher SL, McCormick NH, Velasquez V and Lopez V, Zinc in Specialized Secretory Tissues: Roles in the Pancreas, Prostate, and Mammary Gland, Adv Nutr, 2011, 2, 101–111. [PubMed: 22332039]
7. McCormick N, Velasquez V, Finney L, Vogt S and Kelleher SL, X-Ray Fluorescence Microscopy Reveals Accumulation and Secretion of Discrete Intracellular Zinc Pools in the Lactating Mouse Mammary Gland, PLOS ONE, 2010, 5, e11078. [PubMed: 20552032]
8. Kelleher SL, Velasquez V, Croxford TP, McCormick NH, Lopez V and MacDavid J, Mapping the Zinc-Transporting System in Mammary Cells: Molecular Analysis Reveals a Phenotype-Dependent Zinc-Transporting Network during Lactation, J. Cell. Physiol, 2012, 227, 1761–1770. [PubMed: 21702047]
9. Ball RK, Friis RR, Schoenenberger CA, Doppler W and Groner B, Prolactin Regulation of Beta-Casein Gene Expression and of a Cytosolic 120-Kd Protein in a Cloned Mouse Mammary Epithelial Cell Line, EMBO J, 1988, 7, 2089–2095. [PubMed: 3416834]
10. Gr M, G.-P. D, C. N, M. Bm, T. D and H. Ne, Differentiation and Survival of HC11 Mammary Epithelial Cells: Diverse Effects of Receptor Tyrosine Kinase-Activating Peptide Growth Factors, Eur J Cell Biol, 1996, 70, 97–105. [PubMed: 8793381]
11. Desrivières S, Prinz T, Castro-Palomino Laria N, Meyer M, Boehm G, Bauer U, Schäfer J, Neumann T, Shemanko C and Groner B, Comparative proteomic analysis of proliferating and functionally differentiated mammary epithelial cells, Mol. Cell Proteomics, 2003, 2, 1039–1054. [PubMed: 12885951]
12. Morrison B and Cutler ML, Mouse Mammary Epithelial Cells form Mammospheres During Lactogenic Differentiation, J Vis Exp, 2009, 32, 1265.

13. Pfaffl MW, A New Mathematical Model for Relative Quantification in Real-Time RT–PCR, Nucleic Acids Res, 2001, 29, e45–e45. [PubMed: 11328886]
14. Kim D, Pertea G, Trapnell C, Pimentel H, Kelley R and Salzberg SL, TopHat2: Accurate Alignment of Transcriptomes in the Presence of Insertions, Deletions and Gene Fusions, Genome Biology, 2013, 14, R36. [PubMed: 23618408]
15. Anders S, Pyl PT and Huber W, HTSeq—a Python Framework to Work with High-Throughput Sequencing Data, Bioinformatics, 2015, 31, 166–169. [PubMed: 25260700]
16. Love MI, Huber W and Anders S, Moderated Estimation of Fold Change and Dispersion for RNA-Seq Data with DESeq2, Genome Biology, 2014, 15, 550. [PubMed: 25516281]
17. Fiedler BL, Van Buskirk S, Carter KP, Qin Y, Carpenter MC, Palmer AE and Jimenez R, Droplet Microfluidic Flow Cytometer For Sorting On Transient Cellular Responses Of Genetically-Encoded Sensors, Anal. Chem, 2017, 89, 711–719. [PubMed: 27959493]
18. Cella N, Cornejo-Uribe RR, Montes GS, Hynes NE and Chammas R, The Lysosomal-Associated Membrane Protein LAMP-1 Is a Novel Differentiation Marker for HC11 Mouse Mammary Epithelial Cells, Differentiation, 1996, 61, 113–120. [PubMed: 8983177]
19. Chammas R, Taverna D, Cella N, Santos C and Hynes NE, Laminin and Tenascin Assembly and Expression Regulate HC11 Mouse Mammary Cell Differentiation, J Cell Sci, 1994, 107, 1031–1040. [PubMed: 7520040]
20. T. D, G. B and H. Ne, Epidermal Growth Factor Receptor, Platelet-Derived Growth Factor Receptor, and c-ErbB-2 Receptor Activation All Promote Growth but Have Distinctive Effects upon Mouse Mammary Epithelial Cell Differentiation, Cell Growth Differ, 1991, 2, 145–154. [PubMed: 1676295]
21. Danielson KG, Oborn CJ, Durban EM, Butel JS and Medina D, Epithelial Mouse Mammary Cell Line Exhibiting Normal Morphogenesis in Vivo and Functional Differentiation in Vitro, PNAS, 1984, 81, 3756–3760. [PubMed: 6587390]
22. Cella N, Groner B and Hynes NE, Characterization of Stat5a and Stat5b Homodimers and Heterodimers and Their Association with the Glucocortiocoid Receptor in Mammary Cells, Mol. Cell. Biol, 1998, 18, 1783–1792. [PubMed: 9528750]
23. Maret W, Zinc in Cellular Regulation: The Nature and Significance of “Zinc Signals”, Int J Mol Sci, 2017, 18(11), 2285.
24. Guo L, Lichten LA, Ryu M-S, Liuzzi JP, Wang F and Cousins RJ, STAT5-Glucocorticoid Receptor Interaction and MTF-1 Regulate the Expression of ZnT2 (Slc30a2) in Pancreatic Acinar Cells, Proc. Natl. Acad. Sci. U.S.A, 2010, 107, 2818–2823. [PubMed: 20133611]
25. Jeong J, Walker JM, Wang F, Park JG, Palmer AE, Giunta C, Rohrbach M, Steinmann B and Eide DJ, Promotion of Vesicular Zinc Efflux by ZIP13 and Its Implications for Spondylocheiro Dysplastic Ehlers–Danlos Syndrome, Proc Natl Acad Sci U S A, 2012, 109, E3530–E3538. [PubMed: 23213233]
26. Liuzzi JP, Lichten LA, Rivera S, Blanchard RK, Aydemir TB, Knutson MD, Ganz T and Cousins RJ, Interleukin-6 Regulates the Zinc Transporter Zip14 in Liver and Contributes to the Hypozincemia of the Acute-Phase Response, PNAS, 2005, 102, 6843–6848. [PubMed: 15863613]
27. Kim J-H, Jeon J, Shin M, Won Y, Lee M, Kwak J-S, Lee G, Rhee J, Ryu J-H, Chun C-H and Chun J-S, Regulation of the Catabolic Cascade in Osteoarthritis by the Zinc-ZIP8-MTF1 Axis, Cell, 2014, 156, 730–743. [PubMed: 24529376]
28. Doppler W, Villunger A, Jennewein P, Brduscha K, Groner B and Ball RK, Lactogenic hormone and cell type-specific control of the whey acidic protein gene promoter in transfected mouse cells, Mol Endocrinol, 1991, 5, 1624–1632. [PubMed: 1685765]
29. Lechner J, Welte T, Tomasi JK, Bruno P, Cairns C, Gustafsson J and Doppler W, Promoter-dependent synergy between glucocorticoid receptor and Stat5 in the activation of beta-casein gene transcription, J. Biol. Chem, 1997, 272, 20954–20960. [PubMed: 9252424]
30. Mukhopadhyay SS, Wyszomierski SL, Gronostajski RM and Rosen JM, Differential interactions of specific nuclear factor I isoforms with the glucocorticoid receptor and STAT5 in the cooperative regulation of WAP gene transcription, Mol. Cell. Biol, 2001, 21, 6859–6869. [PubMed: 11564870]
31. LaRochelle O, Labbé S, Harrisson J-F, Simard C, Tremblay V, St-Gelais G, Govindan MV and Séguin C, Nuclear factor-1 and metal transcription factor-1 synergistically activate the mouse

metallothionein-1 gene in response to metal ions, J. Biol. Chem, 2008, 283, 8190–8201. [PubMed: 18230604]

32. Williams C, Helguero L, Edvardsson K, Haldosén L-A and Gustafsson J-Å, Gene Expression in Murine Mammary Epithelial Stem Cell-like Cells Shows Similarities to Human Breast Cancer Gene Expression, Breast Cancer Res, 2009, 11, R26. [PubMed: 19426500]
33. Wang W, Jose C, Kenney N, Morrison B and Cutler ML, Global Expression Profiling Reveals Regulation of CTGF/CCN2 during Lactogenic Differentiation, J Cell Commun Signal, 2009, 3, 43–55. [PubMed: 19353304]
34. Sornapudi TR, Nayak R, Guthikonda PK, Pasupulati AK, Kethavath S, Uppada V, Mondal S, Yellaboina S and Kurukuti S, Comprehensive Profiling of Transcriptional Networks Specific for Lactogenic Differentiation of HC11 Mammary Epithelial Stem-like Cells, Sci Rep, 2018, 8, 11777. [PubMed: 30082875]
35. Diril MK, Ratnacaram CK, Padmakumar VC, Du T, Wasser M, Coppola V, Tessarollo L and Kaldis P, Cyclin-dependent kinase 1 (Cdk1) is essential for cell division and suppression of DNA re-replication but not for liver regeneration, Proc Natl Acad Sci U S A, 2012, 109, 3826–3831. [PubMed: 22355113]
36. Yonekura S, Tsuchiya M, Tokutake Y, Mizusawa M, Nakano M, Miyaji M, Ishizaki H and Haga S, The Unfolded Protein Response Is Involved in Both Differentiation and Apoptosis of Bovine Mammary Epithelial Cells, J. Dairy Sci, 2018, 101, 3568–3578. [PubMed: 29428758]
37. Invernizzi G, Naeem A and Loor JJ, Short Communication: Endoplasmic Reticulum Stress Gene Network Expression in Bovine Mammary Tissue during the Lactation Cycle1, Journal of Dairy Science, 2012, 95, 2562–2566. [PubMed: 22541483]
38. Tsuchiya M, Koizumi Y, Hayashi S, Hanaoka M, Tokutake Y and Yonekura S, The Role of Unfolded Protein Response in Differentiation of Mammary Epithelial Cells, Biochem. Biophys. Res. Commun, 2017, 484, 903–908. [PubMed: 28189674]
39. Qian L, Lopez V, Seo YA and Kelleher SL, Prolactin Regulates ZNT2 Expression through the JAK2/STAT5 Signaling Pathway in Mammary Cells, Am J Physiol Cell Physiol, 2009, 297, C369–C377. [PubMed: 19494234]
40. Lopez V and Kelleher SL, Zinc Transporter-2 (ZnT2) Variants Are Localized to Distinct Subcellular Compartments and Functionally Transport Zinc, Biochemical Journal, 2009, 422, 43–52. [PubMed: 19496757]
41. McCormick NH and Kelleher SL, ZnT4 Provides Zinc to Zinc-Dependent Proteins in the Trans-Golgi Network Critical for Cell Function and Zn Export in Mammary Epithelial Cells, Am J Physiol Cell Physiol, 2012, 303, C291–C297. [PubMed: 22621784]
42. Kelleher SL and Lönnerdal B, Zip3 Plays a Major Role in Zinc Uptake into Mammary Epithelial Cells and Is Regulated by Prolactin, American Journal of Physiology-Cell Physiology, 2005, 288, C1042–C1047. [PubMed: 15634741]
43. Huang L and Gitschier J, A novel gene involved in zinc transport is deficient in the lethal milk mouse, Nat. Genet, 1997, 17, 292–297. [PubMed: 9354792]
44. Ackland ML and Michalczyk A, Zinc deficiency and its inherited disorders -a review, Genes Nutr, 2006, 1, 41–49. [PubMed: 18850219]
45. Cristea S and Polyak K, Dissecting the Mammary Gland One Cell at a Time, Nat Commun, 2018, 9, 1–3. [PubMed: 29317637]
46. Han Y, Goldberg JM, Lippard SJ and Palmer AE, Superiority of SpiroZin2 Versus FluoZin-3 for Monitoring Vesicular Zn2+ Allows Tracking of Lysosomal Zn2+ Pools, Sci Rep, 2018, 8, 1–15. [PubMed: 29311619]
47. Christensen LFB, Malmos KG, Christiansen G and Otzen DE, A Complex Dance: The Importance of Glycosaminoglycans and Zinc in the Aggregation of Human Prolactin, Biochemistry, 2016, 55, 3674–3684. [PubMed: 27305175]
48. Sankoorikal B-J, Zhu YL, Hodsdon ME, Lolis E and Dannies PS, Aggregation of human wild-type and H27A-prolactin in cells and in solution: roles of Zn(2+), Cu(2+), and pH, Endocrinology, 2002, 143, 1302–1309. [PubMed: 11897686]

49. Lu J, Stewart AJ, Sadler PJ, Pinheiro TJT and Blindauer CA, Albumin as a zinc carrier: properties of its high-affinity zinc-binding site, Biochem. Soc. Trans, 2008, 36, 1317–1321. [PubMed: 19021548]
50. Masuoka J, Hegenauer J, Van Dyke BR and Saltman P, Intrinsic stoichiometric equilibrium constants for the binding of zinc(II) and copper(II) to the high affinity site of serum albumin, J. Biol. Chem, 1993, 268, 21533–21537. [PubMed: 8408004]
51. Permyakov EA, Veprintsev DB, Deikus GY, Permyakov SE, Kalinichenko LP, Grishchenko VM and Brooks CL, pH-induced transition and Zn^{2+}-binding properties of bovine prolactin, FEBS Letters, 1997, 405, 273–276. [PubMed: 9108303]
52. Wang C, Liu Y and Cao J-M, Protein-Coupled Receptors: Extranuclear Mediators for the Non-Genomic Actions of Steroids, Int J Mol Sci, 2014, 15, 15412–15425. [PubMed: 25257522]
53. Stahn C and Buttgereit F, Genomic and Nongenomic Effects of Glucocorticoids, Nature Reviews Rheumatology, 2008, 4, 525–533. [PubMed: 18762788]
54. Tasker JG, Di S and Malcher-Lopes R, Minireview: Rapid Glucocorticoid Signaling via Membrane-Associated Receptors, Endocrinology, 2006, 147, 5549–5556. [PubMed: 16946006]
55. Dindia L, Faught E, Leonenko Z, Thomas R and Vijayan MM, Rapid Cortisol Signaling in Response to Acute Stress Involves Changes in Plasma Membrane Order in Rainbow Trout Live, Am. J. Physiol. Endocrinol. Metab., 2013, 304, E1157–1166. [PubMed: 23531621]
56. Gupta N and Mayer D, Interaction of JAK with steroid receptor function, Jakstat, 2013, 2, e24911. [PubMed: 24416641]
57. Kim M-H, Aydemir TB, Kim J and Cousins RJ, Hepatic ZIP14-Mediated Zinc Transport Is Required for Adaptation to Endoplasmic Reticulum Stress, Proc. Natl. Acad. Sci. U.S.A, 2017, 114, E5805–E5814. [PubMed: 28673968]
58. Kim M-H, Aydemir TB and Cousins RJ, Zinc and ZIP14 (Slc39a14) Are Required for Adaptation to ER Stress in Mouse Liver, The FASEB Journal, 2016, 30, 148.2–148.2.
59. Homma K, Fujisawa T, Tsuburaya N, Yamaguchi N, Kadowaki H, Takeda K, Nishitoh H, Matsuzawa A, Naguro I and Ichijo H, SOD1 as a Molecular Switch for Initiating the Homeostatic ER Stress Response under Zinc Deficiency, Mol. Cell, 2013, 52, 75–86. [PubMed: 24076220]
60. Colston KW, Berger U, Wilson P, Hadcocks L, Naeem I, Earl HM and Coombes RC, Mammary Gland 1, 25-Dihydroxyvitamin D3 Receptor Content during Pregnancy and Lactation, Molecular and Cellular Endocrinology, 1988, 60, 15–22. [PubMed: 2850946]
61. de O F. Andrade, S. de Assis, L. Jin, C. C. Fontelles, L. F. Barbisan, E. Purgatto, L. Hilakivi-Clarke and T. P. Ong, Lipidomic Fatty Acid Profile and Global Gene Expression Pattern in Mammary Gland of Rats That Were Exposed to Lard-Based High Fat Diet during Fetal and Lactation Periods Associated to Breast Cancer Risk in Adulthood, Chemico-Biological Interactions, 2015, 239, 118–128. [PubMed: 26115784]
62. Goddio MV, Gattelli A, Tocci JM, Cuervo LP, Stedile M, Stumpo DJ, Hynes NE, Blackshear PJ, Meiss RP and Kordon EC, Expression of the MRNA Stability Regulator Tristetraprolin Is Required for Lactation Maintenance in the Mouse Mammary Gland, Oncotarget, 2018, 9, 8278–8289. [PubMed: 29492194]
63. Goddio MV, Gattelli A, Slomiansky V, Lacunza E, Gingerich T, Tocci JM, Facchinetti MM, Curino AC, LaMarre J, Abba MC and Kordon EC, Mammary Differentiation Induces Expression of Tristetraprolin, a Tumor Suppressor AU-Rich MRNA-Binding Protein, Breast Cancer Research and Treatment, 2012, 135, 749–758. [PubMed: 22968621]
64. Fairhurst A-M, Connolly JE, Hintz KA, Goulding NJ, Rassias AJ, Yeager MP, Rigby W and Wallace PK, Regulation and Localization of Endogenous Human Tristetraprolin, Arthritis Res Ther, 2003, 5, R214–R225. [PubMed: 12823857]

Significance to Metallomics

In this manuscript we take a global approach to examine how transformation from a proliferative to a differentiated secretory state alters zinc levels, zinc regulatory genes, and zinc dependent pathways in mammary epithelial cells. This work provides insight into how epithelial cells remodel zinc homeostasis during lactation while also shedding light on the regulation of zinc transporters themselves.

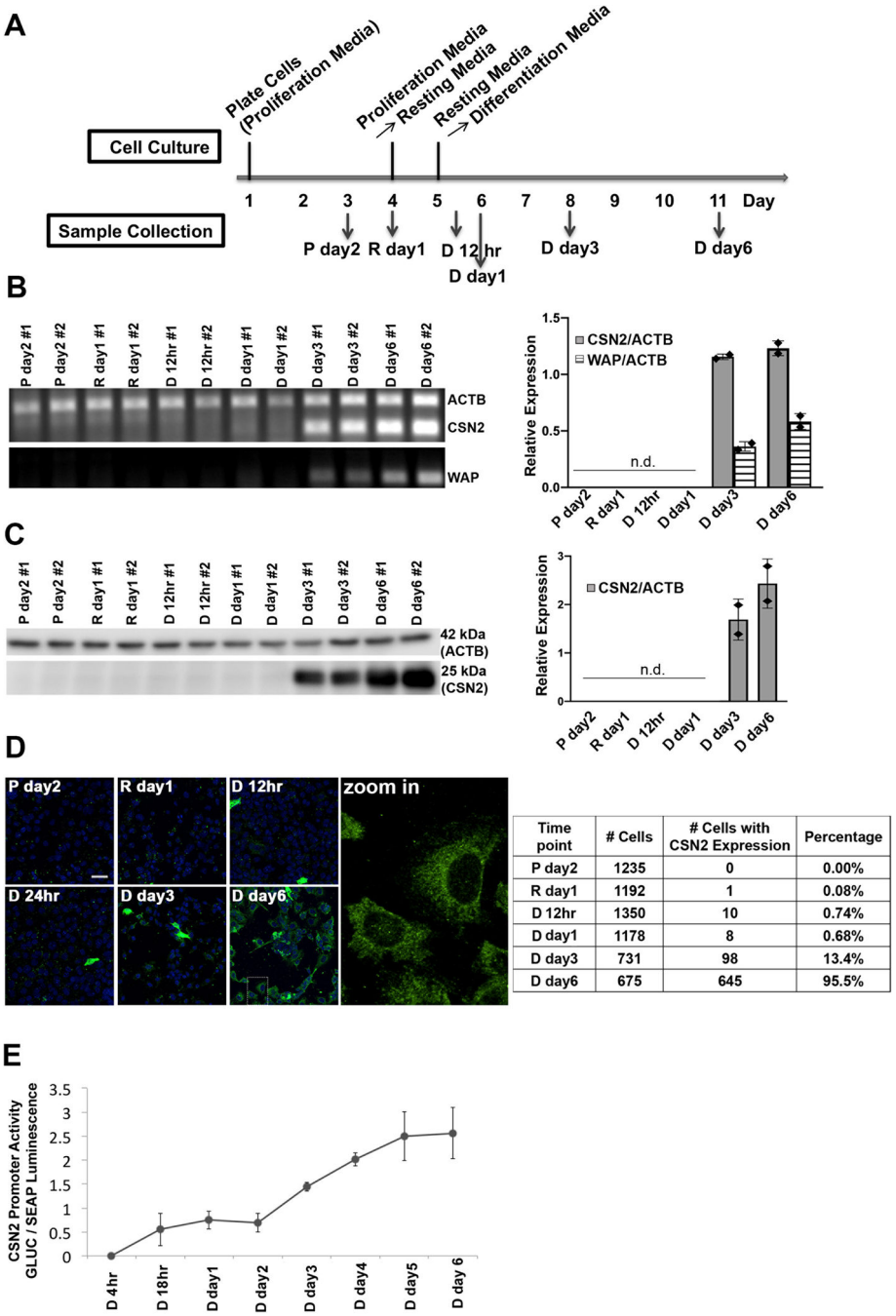

Time point	# Cells	# Cells with CSN2 Expression	Percentage
P day2	1235	0	0.00%
R day1	1192	1	0.08%
D 12hr	1350	10	0.74%
D day1	1178	8	0.68%
D day3	731	98	13.4%
D day6	675	645	95.5%

Figure 1: Characterization of HC11 cell differentiation upon hormone treatment.

(A) Outline of the differentiation protocol (P, proliferation media; R, resting media; D, differentiation media). (B) RT-PCR of control gene actin (ACTB) and differentiation markers casein (CSN2) and whey acid protein (WAP). Left: Agarose gel showing intensity of PCR signal over the course of differentiation; Right: mean values of relative expression of CSN2 and WAP normalized to ACTB. n.d., not detected. Each diamond represents a biological replicate. (C) Immunoblot of CSN2 and ACTB protein expression at different time points. Left: SDS-PAGE blot and Right: mean values of relative protein expression

(CSN2 normalized to ACTB). n.d., not detected. Each diamond represents a biological replicate. (D) Immunofluorescence of casein protein expression at the single cell level. Left: representative fluorescence images. Green: CSN2; Blue: Nucleus. Scale bar, 40 μm. Right: Quantification of immunofluorescence. Percentages represent cells with CSN2 expression divided by the total cell number. Counts are from 2 independent experiments. (E) Dual luciferase reporter assay of the transcriptional activity of the CSN2 promoter at different time points post hormone treatment. The Gaussia Luciferase (GLUC) signal was normalized to the signal of the constitutively expressed secreted alkaline phosphatase (SEAP) (n = 2). Error bars represent standard deviation.

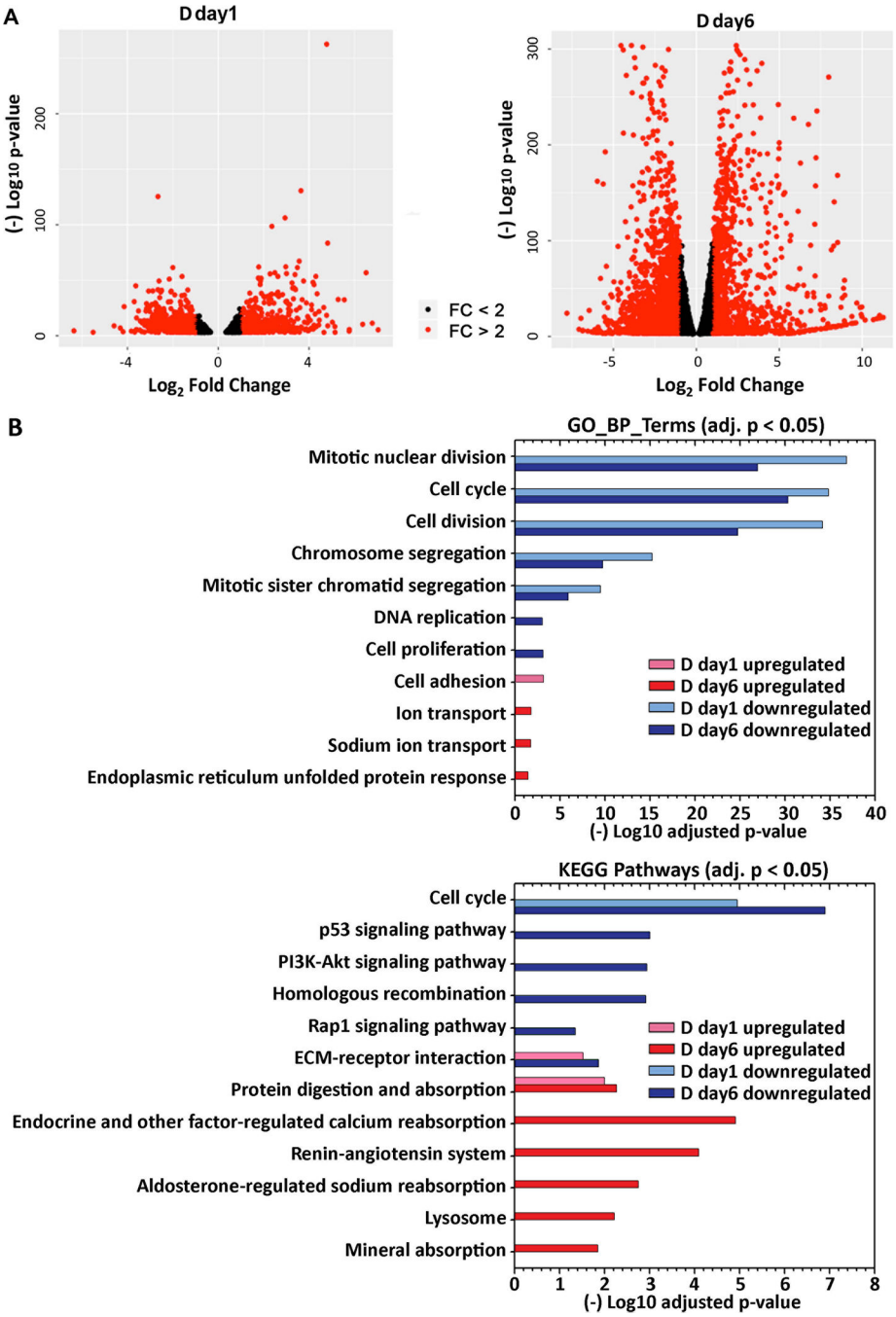

Figure 2. Global differential expression at day 1 and day 6 post hormone treatment.

(A) Differentially expressed genes identified from DEseq2 ($p_{adj} < 0.001$), as plotted in volcano plots. Genes upregulated or downregulated with fold change > 2 are labeled as red dots. (B) Functional annotation of upregulated and downregulated genes was performed using DAVID GOTERM_BP_DIRECT or KEGG pathway annotations. Select GO terms (adjusted $p < 0.05$) or KEGG pathways (adjusted $p < 0.05$) in either the D day1 or D day6 samples are visualized in the bar plot.

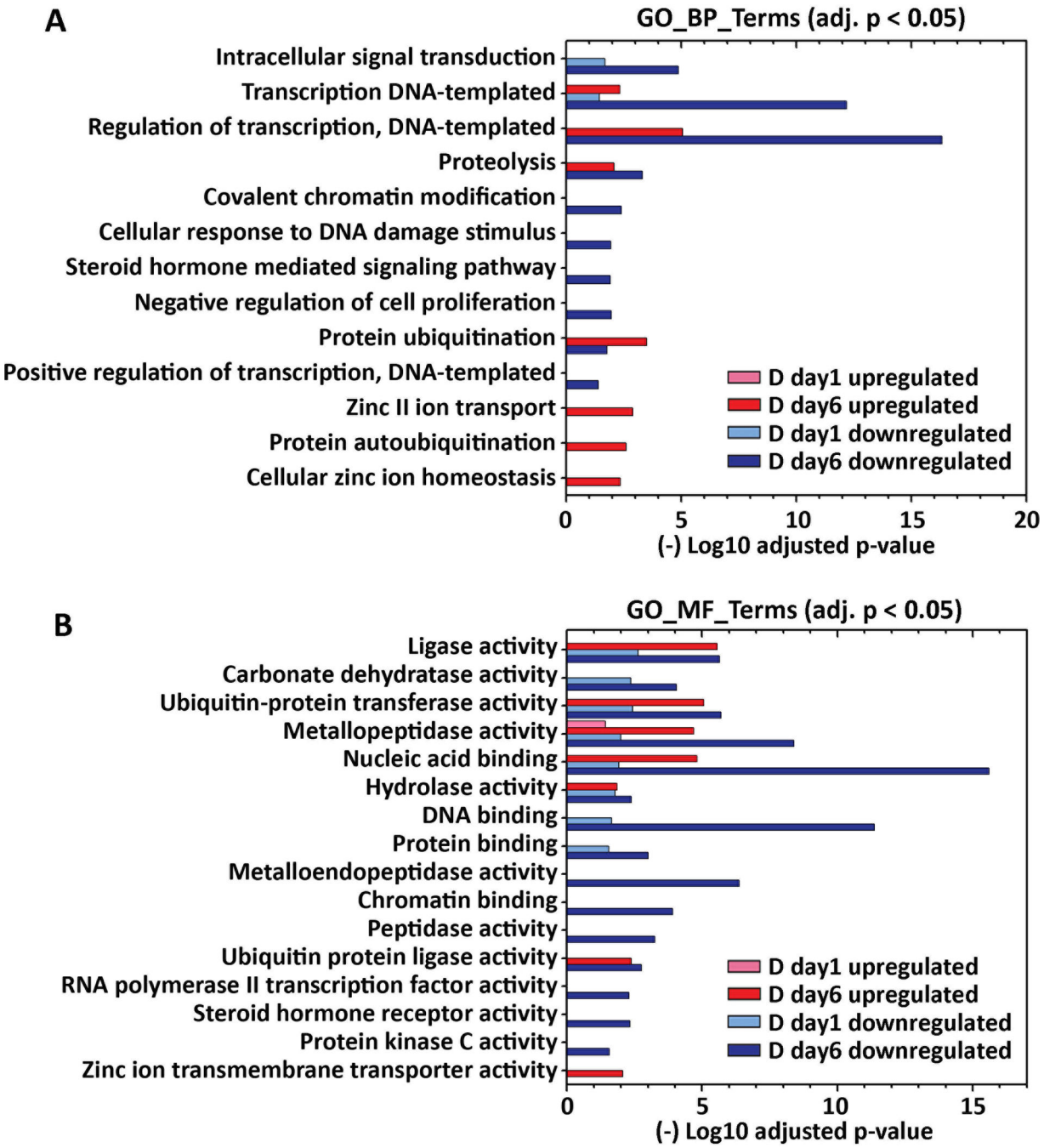

Figure 3. Gene Ontology functional enrichment of zinc-dependent genes differentially expressed at day 1 and day 6 post hormone treatment.

Analysis of functional annotations of upregulated and downregulated zinc-dependent genes (DEseq2: fold change > 1.5 and $p_{adj} < 0.001$) was performed using DAVID with GOTERM_BP_DIRECT (A) and GOTERM_MF_DIRECT (B) annotations. Enriched GO terms (adjusted $p < 0.05$) in either D day1 or D day6 sample are visualized in the bar plot.

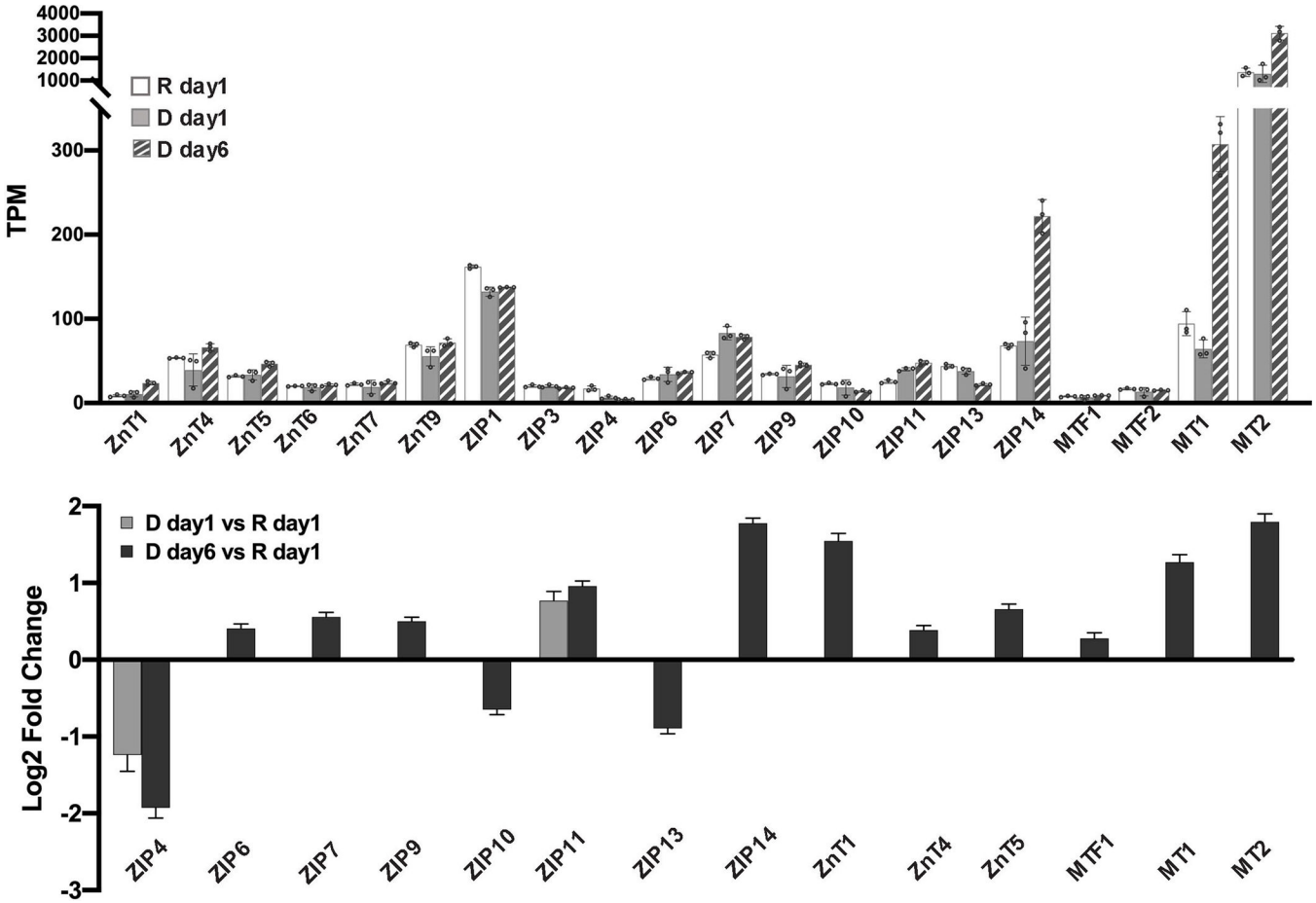

Figure 4. Differential expression of zinc homeostasis genes.

(A) Mean TPM values from 3 independent biological replicates for zinc homeostasis genes under resting and differentiated conditions. Each dot represents a biological replicate. Error bars represent standard deviation among 3 biological replicates. (B) Mean log2(Fold Change) of differentially expressed zinc homeostasis genes upon hormone treatment normalized to expression under resting conditions. Only genes with mean TPM > 1 are included. Differential expression was analyzed using DESeq2, $p_{adj} < 0.001$. Error bars represent lfcSE (log fold change Standard Error) among 3 biological replicates.

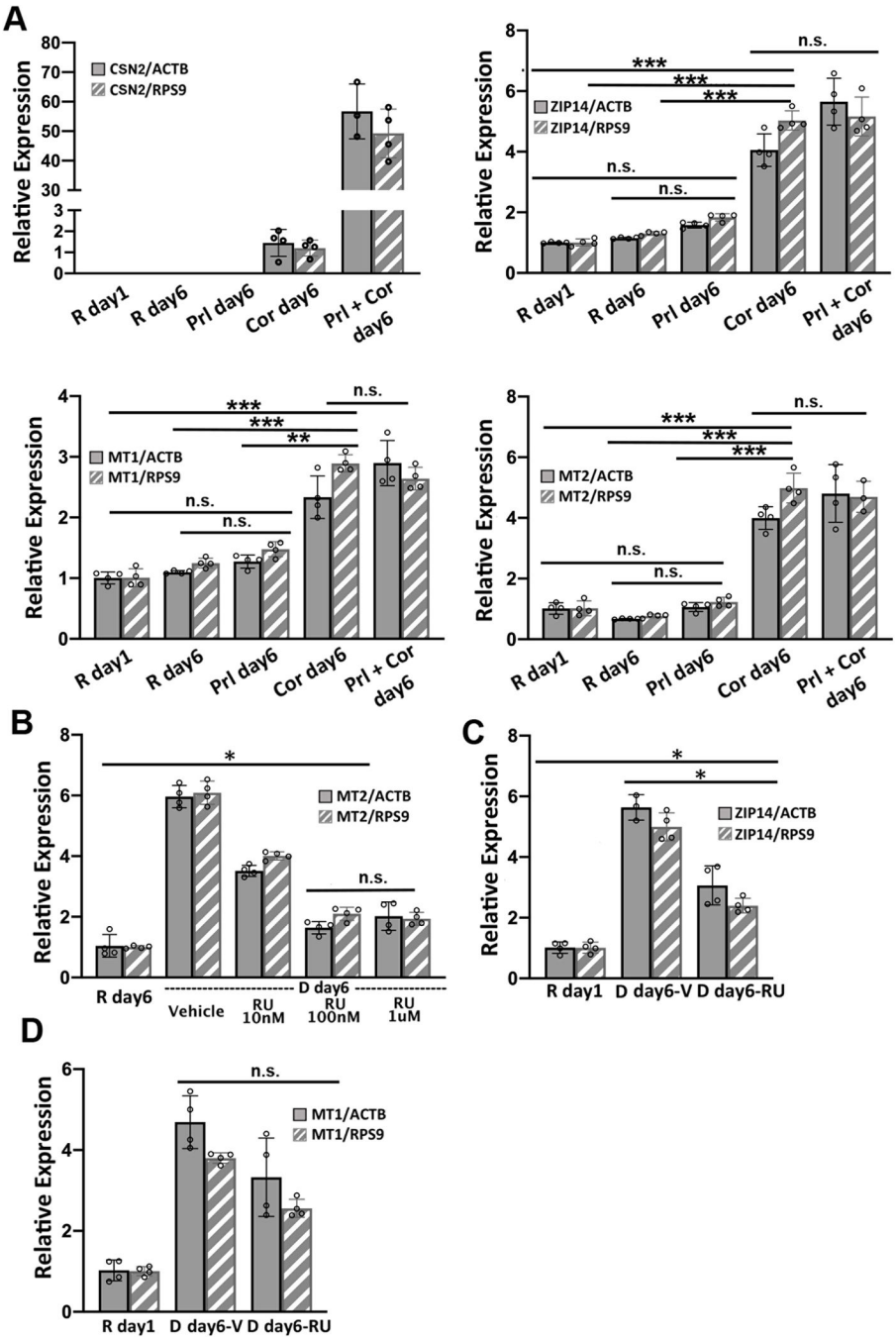

Figure 5. Hydrocortisone increases the steady-state level of ZIP14, MT1 and MT2 mRNAs.

(A) RT-qPCR of CSN2, ZIP14, MT1 and MT2 normalized to either ACTB or RSP9 reference genes. ** $p < 0.0002$, *** $p < 0.0001$, unpaired student's t-test (n=4). (B) RT-qPCR of MT2 normalized to either ACTB or RSP9 in resting media or differentiation media in the presence or absence of different concentrations of the glucocorticoid receptor antagonist RU486 (RU). (C-D) RT-qPCR of ZIP14 (C) and MT1 (D) normalized to either ACTB or RSP9 in resting media or differentiation media with 100 nM RU or vehicle (V) control. * $p < 0.01$, unpaired student's t-test (n=4). For MT1, RU treatment did not

significantly affect the mRNA level. Each dot represents a biological replicate. Error bars represent standard deviation.

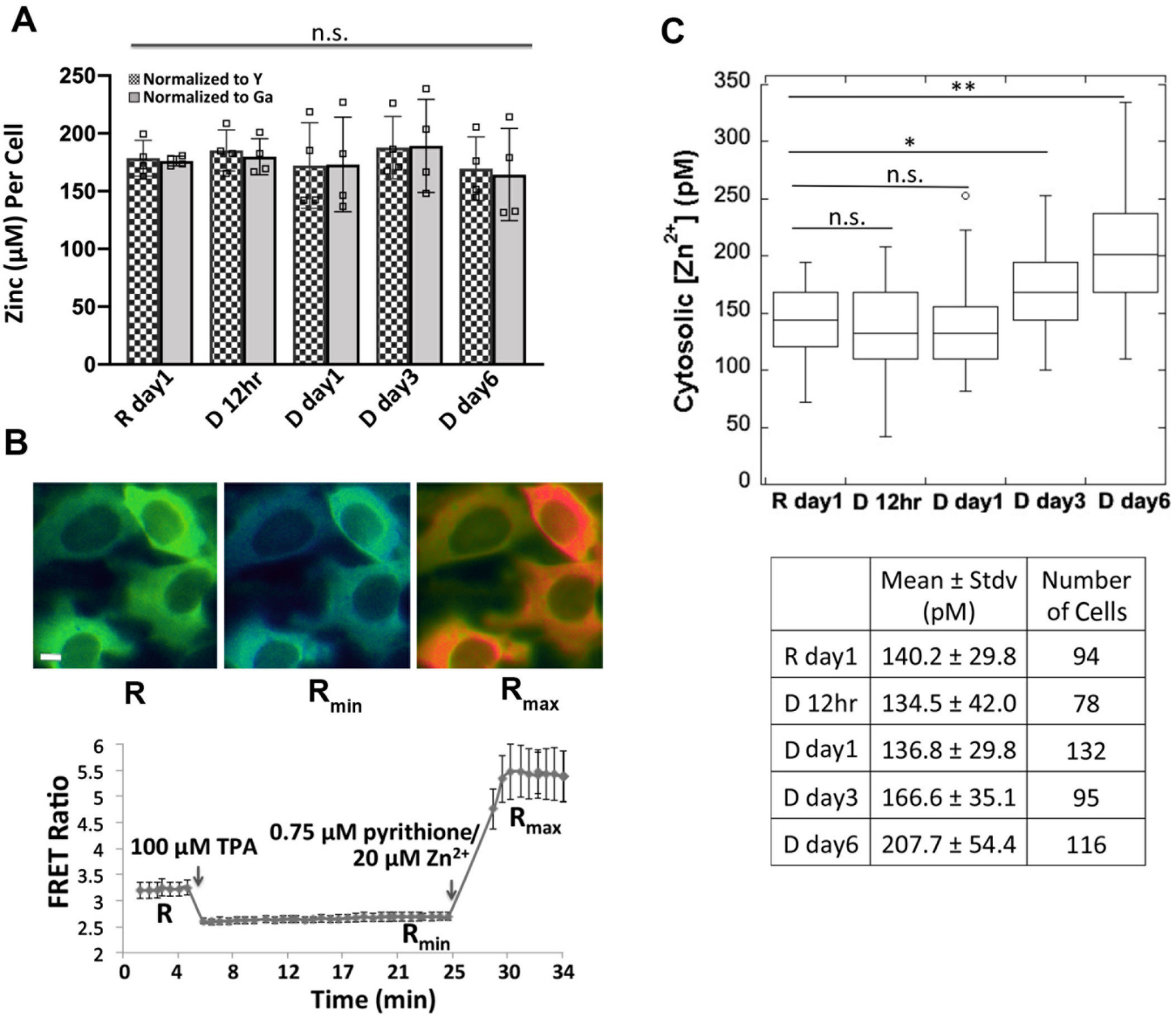

	Mean ± Stdv (pM)	Number of Cells
R day1	140.2 ± 29.8	94
D 12hr	134.5 ± 42.0	78
D day1	136.8 ± 29.8	132
D day3	166.6 ± 35.1	95
D day6	207.7 ± 54.4	116

Figure 6. Measurement of total zinc and labile cytosolic Zn^{2+} over the progression of cell differentiation.

(A) Quantification of the mean of total zinc (n=4) by ICP-MS. The ppb zinc in each sample was normalized to the ppb of a spike-in control Yttrium (Y) or Gallium (Ga) and then converted to concentration per cell. Each square represents a biological replicate. n.s. not significant, one-way ANOVA test with Post Hoc Tukey HSD (n=4). (B) Pseudo-colored fluorescence ratio images (FRET / CFP) of HC11 cells expressing the NES-ZapCV2 sensor (top) and FRET ratio in the cytosol as a function of *in situ* calibration (bottom). Images represent the resting state (R), post TPA treatment (R_{min}) and post pyrithione/Zn^{2+} treatment (R_{max}). Scale bar, 10 μm. Data represent mean ± stdv of 10 cells. (C) Quantification of cytosolic labile Zn^{2+} over the progression of differentiation reveals that Zn^{2+} increases at day 3 and day 6 post hormone treatment. The distribution of data is shown in a box plot with

the ends of the box representing the upper and lower quartiles. * $p < 0.0005$; ** $p < 0.0001$, one-way ANOVA test.

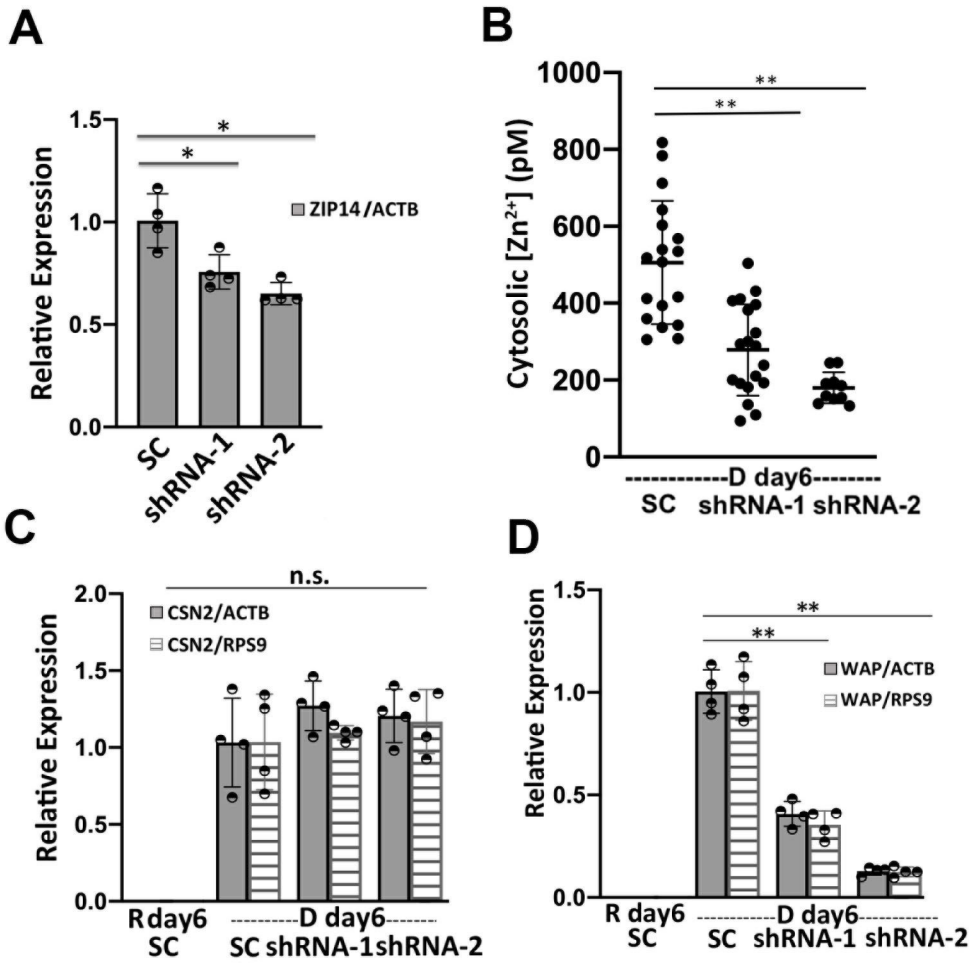

Figure 7. ZIP14 increases cytosolic Zn^{2+} at D day6 and activates WAP mRNA expression.

(A) The relative expression of ZIP14 normalized to ACTB in ZIP14 knockdown (KD) cells expressing two different shRNAs compared to scrambled control shRNA. (B) Cytosolic Zn^{2+} concentration in ZIP14 KD cells compared to control cells at 6 days post hormone treatment. Each dot represents a single cell and black line represents the mean value of each group. Error bar represents standard deviation. **, p< 0.0001, one-way ANOVA test with Post Hoc Tukey HSD (n > 9). (C-D) ZIP14 knockdown depressed the mRNA expression of WAP (D) but had no effect in the CSN2 mRNA level (C) in D day6 cells. Relative mRNA level in (A, C, D) was determined using RT-qPCR and mean values are represented by bar plots with each dot representing a biological replicate. *, P < 0.05; **, p < 0.001, unpaired student's t-test (n=4).